CLASSIFICATION OF HYPERSPECTRAL IMAGES BASED ON CONVOLUTIONAL NEURAL NETWORKS AND SPECTRAL UNMIXING

ENG. JHON EDWARD PINTO BARRERA

UNIVERSIDAD INDUSTRIAL DE SANTANDER
FACULTAD DE INGENIERÍAS FISICOMECÁNICAS
ESCUELA DE INGENIERÍA DE SISTEMAS E INFORMÁTICA
BUCARAMANGA
2020

CLASSIFICATION OF HYPERSPECTRAL IMAGES BASED ON CONVOLUTIONAL NEURAL NETWORKS AND SPECTRAL UNMIXING

ENG. JHON EDWARD PINTO BARRERA

Trabajo de Grado para optar al título de
Magister en Ingeniería de Sistemas

Advisor
Ph.D Henry Arguello Fuentes
Co-advisor
Ph.D Juan Marcos Ramírez Rondon

UNIVERSIDAD INDUSTRIAL DE SANTANDER
FACULTAD DE INGENIERÍAS FISICOMECÁNICAS
ESCUELA DE INGENIERÍA DE SISTEMAS E INFORMÁTICA
BUCARAMANGA
2020

ACTA DE SUSTENTACIÓN
TRABAJO DE INVESTIGACIÓN DE MAESTRÍA EN INGENIERÍA DE SISTEMAS E INFORMÁTICA

Universidad Industrial de Santander

De acuerdo con el artículo 109 del Reglamento General de Posgrado (Acuerdo del Consejo Superior No 075 de 2013), los suscritos miembros del jurado del Trabajo de Investigación de Maestría **"Classification of Hyperspectral Images based on Convolutional Neural Networks and Spectral Unmixing"** presentado por el estudiante de Maestría en Ingeniería de Sistemas e Informática **Jhon Edward Pinto Barrera**, código **2188271** una vez evaluada y realizada la defensa oral dan concepto de:

APROBADO [X] **NO APROBADO** [ ] **APLAZADO** [ ]

Se envía comunicación escrita de la presente decisión tanto al estudiante como a su director a los 9 días del mes de diciembre de 2020.

Prof. **HENRY ARGÜELLO FUENTES** (EISI-UIS).
Director del Trabajo de Investigación de Maestría

Prof. **JUAN MARCOS RAMÍREZ RONDÓN** (Universidad Rey Juan Carlos)
Co-Director del Trabajo de Investigación de Maestría

Prof. **SAID DAVID PERTUZ ARROYO** (E3T-UIS).
Evaluador.

Prof. **FERLEY MEDINA ROJAS** (Universidad SurColombiana-Neiva).
Evaluador.

COORDINACIÓN DE PROGRAMAS DE POSGRADOS
ESCUELA DE INGENIERÍA DE SISTEMAS E INFORMÁTICA
Edificio Facultad de Ingenierías Fisico-mecanicas
PBX: (7) 6344000 Ext. 2481 FAX: 6349042 A.A. 678 Bucaramanga, Colombia
Correo-e: maesinfo@uis.edu.co

ACREDITACIÓN INSTITUCIONAL

ENTREGA DE TRABAJOS DE GRADO, TRABAJOS DE INVESTIGACION O TESIS Y AUTORIZACIÓN DE SU USO A FAVOR DE LA UIS

Yo, JHON EDWARD PINTO BARRERA, mayor de edad, vecino de Bucaramanga, identificado con la Cédula de Ciudadanía No. 1095820955 de Floridablanca, actuando en nombre propio, en mi calidad de autor del trabajo de grado, del trabajo de investigación, o de la tesis denominada(o):

CLASSIFICATION OF HYPERSPECTRAL IMAGES BASED ON CONVOLUTIONAL NEURAL NETWORKS AND SPECTRAL UNMIXING,

hago entrega del ejemplar respectivo y de sus anexos de ser el caso, en formato digital o electrónico (CD o DVD) y autorizo a LA UNIVERSIDAD INDUSTRIAL DE SANTANDER, para que en los términos establecidos en la Ley 23 de 1982, Ley 44 de 1993, decisión Andina 351 de 1993, Decreto 460 de 1995 y demás normas generales sobre la materia, utilice y use en todas sus formas, los derechos patrimoniales de reproducción, comunicación pública, transformación y distribución (alquiler, préstamo público e importación) que me corresponden como creador de la obra objeto del presente documento. PARÁGRAFO: La presente autorización se hace extensiva no sólo a las facultades y derechos de uso sobre la obra en formato o soporte material, sino también para formato virtual, electrónico, digital, óptico, uso en red, Internet, extranet, intranet, etc., y en general para cualquier formato conocido o por conocer.

EL AUTOR – ESTUDIANTE, manifiesta que la obra objeto de la presente autorización es original y la realizó sin violar o usurpar derechos de autor de terceros, por lo tanto la obra es de su exclusiva autoría y detenta la titularidad sobre la misma. PARÁGRAFO: En caso de presentarse cualquier reclamación o acción por parte de un tercero en cuanto a los derechos de autor sobre la obra en cuestión, EL AUTOR / ESTUDIANTE, asumirá toda la responsabilidad, y saldrá en defensa de los derechos aquí autorizados; para todos los efectos la Universidad actúa como un tercero de buena fe.

Para constancia se firma el presente documento en dos (02) ejemplares del mismo valor y tenor, en Bucaramanga, a los 10 días del mes de diciembre de Dos Mil veinte 2020.

EL AUTOR / ESTUDIANTE:

Jhon Edward Pinto Barrera

DEDICATORIA

A Dios por haberme dado vida y salud para culminar esta etapa. A mi madre, por ser una mujer luchadora, por enseñarme a caminar por la vida, por brindarme su amor incondicional, por exigirme y motivarme a ser cada día mejor y por ser ese gran apoyo excepcional. A todos mis amigos y familiares que fueron parte de este gran logro, por acompañarme en cada momento y depositarme su confianza.

AGRADECIMIENTOS

Al profesor Juan Marcos Ramírez por su dedicación, paciencia y valiosos aportes en mi formación, por demostrarme que con esfuerzo cualquier meta se puede cumplir. Al profesor Henry Arguello por permitirme formar parte de su grupo de investigación, por depositarme su voto de confianza y por todas sus enseñanzas. A Jenifer Suárez, mi compañera de trayecto, por su constante apoyo, compañía y motivación.

CONTENIDO

LISTA DE FIGURAS

LISTA DE TABLAS

pág.

RESUMEN

TITULO: CLASSIFICATION OF HYPERSPECTRAL IMAGES BASED ON CONVOLUTIONAL NEURAL NETWORKS AND SPECTRAL UNMIXING *

AUTOR: JHON EDWARD PINTO BARRERA **

PALABRAS CLAVES: Imágenes Hiperespectrales, Redes Neuronales Convolucionales, Desmezclado Espectral, Clasificación.

DESCRIPCIÓN:

Las imágenes hiperespectrales (HSIs) corresponden a cubos de datos que contienen información espacial de una escena a lo largo del espectro electromagnético. En general, estas imágenes se han usado para identificar diferentes características de las escenas gracias a su alto contenido espectral, estas han favorecido el desarrollo de aplicaciones como, la detección de enfermedades en cultivos y la discriminación de materiales presentes en una escena. En particular, el análisis de las firmas espectrales de diversos tipos de vegetación ha permitido obtener información sobre el estado y el crecimiento de los cultivos agrícolas. En este sentido, la clasificación de HSIs es una tarea desafiante, debido a que, las firmas adquiridas son afectadas por diversos factores, tales como, los cambios en los niveles de iluminación e incertidumbres de los equipos de medición. Además, la mayoría de los métodos de clasificación no consideran la mezcla del contenido espectral de múltiples materiales en un único píxel. Para superar esta limitación, las técnicas de desmezclado espectral han emergido para estimar la contribución de los diferentes materiales en un único píxel. Por otro lado, las redes neuronales convolucionales (CNN) son estructuras de aprendizaje profundo que han demostrado un notable rendimiento en tareas de clasificación de información visual. Estas arquitecturas típicamente están conformadas por capas convolucionales, capa de funciones de activación no lineal, capa de agrupamiento y una capa completamente conectada, que ejecuta la tarea de clasificación multiclase. En este trabajo, se propone un enfoque de clasificación de HSIs mediante el uso de un método de desmezclado espectral y CNN. Específicamente, el método propuesto utiliza los mapas de abundan-

* Trabajo de grado

** Facultad de Ingenierías Fisicomecánicas. Escuela de Ingeniería de Sistemas e Informática. Director: Ph.D Henry Arguello Fuentes, Co-director Ph.D Juan Marcos Ramírez Rondon cia extraídos de una HSI como entrada a una CNN. El propósito de este trabajo es aprovechar las ventajas del desmezclado espectral, incluyendo la descomposición a nivel de sub-píxeles, la reducción de la dimensionalidad y el rendimiento notable de las CNN. El método propuesto se verificó a través de cuatro conjuntos de datos de HSIs tradicionales, como Pavia University, Salinas Valley, Indian y la Oil Palm. Asimismo, el método de clasificación propuesto presenta un mejor rendimiento de clasificación en términos de precisión general comparado con diferentes métodos de clasificación de la literatura, tales como, máquina de soporte vectorial (SVM, del inglés Support Vector Machine), máquina de soporte vectorial con función de base radial (SVM-RBF, del inglés Support Vector Machine - Radial Basis Function) y por último el método de vecinos más cercanos (K-NN, del inglés k-nearest neighbors algorithm).

ABSTRACT

TITLE: CLASSIFICATION OF HYPERSPECTRAL IMAGES BASED ON CONVOLUTIONAL NEURAL NETWORKS AND SPECTRAL UNMIXING *

AUTHOR: JHON EDWARD PINTO BARRERA **

KEYWORDS: Hyperspectral images, convolutional neural networks, spectral unmixing, classification.

DESCRIPTION:

Hyperspectral images (HSIs) correspond to data cubes that contain spatial information of a scene along the electromagnetic spectrum. In general, these images have been used to identify different characteristics of the scenes thanks to its high spectral content, these have favored the development of applications such as, the detection of diseases in crops and the discrimination of materials present in a scene. In particular, the analysis of the spectral signatures of various types of vegetation has made it possible to obtain information on the state and growth of agricultural crops. In this sense, the classification of HSIs is a challenging task, because the acquired signatures are affected by various factors, such as changes in lighting levels and uncertainties of the measurement equipment. In addition, most classification methods do not consider mixing the spectral content of multiple materials into a pixel. To overcome this limitation, spectral unmixing techniques have emerged to estimate the contribution of different materials in a pixel. On the other hand, convolutional neural networks (CNN) have shown a remarkable performance in visual information classification tasks. These architectures typically consist of convolutional layers, a nonlinear activation layer, a pooling layer, and a fully connected layer, which performs the task of multi-class classification. In this paper, a classification approach to HSIs is proposed using a spectral unmixing method and CNN. Specifically, the proposed method uses the abundance maps extracted from an HSI as input to a CNN. The purpose of this work is to take advantage of spectral unmixing, including sub-pixel level decomposition, reduced dimensionality, and remarkable yield of CNNs.The proposed method was verified through four traditional HSI data sets,

---

* Trabajo de grado

** Facultad de Ingenierías Fisicomecánicas. Escuela de Ingeniería de Sistemas e Informática. Advisor: Ph.D Henry Arguello Fuentes, Co-advisor Ph.D Juan Marcos Ramírez Rondon such as Pavia University, Salinas Valley, Indian and Oil Palm. In addition, the proposed classification method presents a better classification performance in terms of overall accuracy compared to different classification methods in the literature, such as Support Vector Machine (SVM), Support Vector Machine - Radial Basis Function (SVM-RBF) and finally the Nearest Neighbors Method (K-NN).

INTRODUCTION

Hyperspectral imaging is a technique that allows the acquisition of information of objects on the Earth's surface. Specifically, this technique acquires the spectral behavior of each pixel within the observed scene at hundreds of wavelength bands[1] range from the visible zone (VIS, 0.4-0.8 um) to the near-infrared region (NIR, 0.8-2.4 um). Furthermore, hyperspectral images (HSIs) have been widely used in several applications such as agriculture[2], environment[3], mining[4], among others.

Nowadays, HSIs are used in classification or detection procedures in order to identify targets or materials in a scene exploiting the ability of the hyperspectral sensors of acquiring spatial and spectral information in different wavelengths of the electromagnetic spectrum[5]. In particular, the HSI classification is one of the most important technological advances at present, where its main aim is to assign a unique label to each spectral pixel, where the selected label belongs to a previously known class[6].

---

1 Gustavo Camps-Valls y col. "Remote sensing image processing". En: *Synthesis Lectures on Image, Video, and Multimedia Processing* 5.1 (2011), págs. 1-192.

2 Lankapalli Ravikanth y col. "Extraction of spectral information from hyperspectral data and application of hyperspectral imaging for food and agricultural products". En: *Food and Bioprocess Technology* 10.1 (2017), págs. 1-33.

3 Sabine Chabrillat y col. "Use of hyperspectral images in the identification and mapping of expansive clay soils and the role of spatial resolution". En: *Remote sensing of Environment* 82.2-3 (2002), págs. 431-445.

4 Enton Bedini y Thorkild M Rasmussen. "Use of airborne hyperspectral and gamma-ray spectroscopy data for mineral exploration at the Sarfartoq carbonatite complex, southern West Greenland". En: *Geosciences Journal* (2018), págs. 1-11.

5 Pedram Ghamisi y col. "Advances in hyperspectral image and signal processing: A comprehensive overview of the state of the art". En: *IEEE Geoscience and Remote Sensing Magazine* 5.4 (2017), págs. 37-78.

6 Gustavo Camps-Valls y col. "Advances in hyperspectral image classification: Earth monitoring

In general, traditional techniques consider every spectral pixel as a classification feature. However, the combination of the spectral responses belonging to different materials covered by a unique pixel, and the low spatial resolution of HSIs severely degrade the performance of the classification methods. Therefore, a classification approach that considers the contribution of the different materials in the formation of the corresponding spectral signature is required.

Nevertheless, in the state-of-the-art, there are other techniques such as those based on spectral unmixing (SU) that decomposes the HSI at sub-pixel level, which promise better results in the classification performance. Specifically, SU is a procedure by which the measured spectrum of a mixed pixel is decomposed into a collection of known spectral signatures (endmembers) that correspond to different materials in the scene, such as water, soil, metal, among others, and a set of corresponding fractions (abundances) that indicate the endmembers proportion contributing to the construction of each spectral pixel[7]. Furthermore, the SU technique significantly reduce the number of elements associated to each spatial coordinate, reducing in turn, the dimensionality of the corresponding HSI feature. Since that the SU decompose the spectral content and reduce the dimensionality of the pixels, we consider the abundance map obtained by a SU technique as an input of the classifier that can improve the labeling accuracy.

On the other hand, one of the most popular deep learning techniques with a high performance in imaging classification tasks is the convolutional neural network (CNN) approach, which consists of extracting deep features from the data under test. CNNs are composed by a set of blocks that can be applied both across space and time signals e.g., images, audio and video signals. In essence, each block contain a set of

---

with statistical learning methods”. En: *IEEE signal processing magazine* 31.1 (2013), págs. 45-54.

[7] Nirmal Keshava y John F Mustard. “Spectral unmixing”. En: *IEEE signal processing magazine* 19.1 (2002), págs. 44-57.

filter masks that are applied to the input data[8] followed by a nonlinear activation function whose output typically serve as input to the next network block. These blocks are part of feature extraction stages, which consist of three layers: 1) a convolutional layer, 2) a non linearity layer and 3) a pooling layer[9]. CNN has achieved to impact in different fields of science such as: human performance[10], image classification[11] [12], object detection[13], scene labeling[14], house numbers digit classification[15], face recognition[16], among others. Therefore, we aim at combining the benefits of both the SU techniques and the powerful and promising CNN tool in spectral image classification

---

[8] ME Paoletti y col. “A new deep convolutional neural network for fast hyperspectral image classification”. En: *ISPRS Journal of Photogrammetry and Remote Sensing* 145 (2018), págs. 120-147.

[9] Liangpei Zhang, Lefei Zhang y Bo Du. “Deep learning for remote sensing data: A technical tutorial on the state of the art”. En: *IEEE Geoscience and Remote Sensing Magazine* 4.2 (2016), págs. 22-40.

[10] Pierre Sermanet y Yann LeCun. “Traffic sign recognition with multi-scale convolutional networks”. En: *Neural Networks (IJCNN), The 2011 International Joint Conference on*. IEEE. 2011, págs. 2809-2813.

[11] Alex Krizhevsky, Ilya Sutskever y Geoffrey E Hinton. “Imagenet classification with deep convolutional neural networks”. En: *Advances in neural information processing systems*. 2012, págs. 1097-1105.

[12] Dan Cireşan, Ueli Meier y Jürgen Schmidhuber. “Multi-column deep neural networks for image classification”. En: *arXiv preprint arXiv:1202.2745* (2012).

[13] Ross Girshick y col. “Rich feature hierarchies for accurate object detection and semantic segmentation”. En: *Proceedings of the IEEE conference on computer vision and pattern recognition*. 2014, págs. 580-587.

[14] Clement Farabet y col. “Learning hierarchical features for scene labeling”. En: *IEEE transactions on pattern analysis and machine intelligence* 35.8 (2013), págs. 1915-1929.

[15] Pierre Sermanet, Soumith Chintala y Yann LeCun. “Convolutional neural networks applied to house numbers digit classification”. En: *Pattern Recognition (ICPR), 2012 21st International Conference on*. IEEE. 2012, págs. 3288-3291.

[16] Yaniv Taigman y col. “Deepface: Closing the gap to human-level performance in face verification”. En: *Proceedings of the IEEE conference on computer vision and pattern recognition*. 2014, págs. 1701-1708.

tasks.

In this work, a hyperspectral image classification technique is proposed that exploits the advantages of both the low-dimensional decomposition of the spectral pixels performed by a SU technique and the representation power of the CNN. Basically, the proposed approach implements the sparse unmixing method via variable splitting augmented Lagrangian and total variation (SunSal-TV)[17] to obtain the respective HSI abundance map. Furthermore, the abundance map patches are considered as data input of a supervised learning machine relied on CNN for performing a pixel-based hyperspectral classification task. The proposed approach is evaluated for four standard HSI databases: Pavia University, Salinas Valley, Indian Pines and Oil Palm. In addition, the performance of the proposed classification method is compared to similar approaches based on traditional machine learning techniques including the nearest neighbor (KNN)[18] method, the support vector machines with linear kernel (SVM), and support vector machines with Gaussian kernel (SVM-RBF)[19]. Numerical simulations show that the proposed classification method outperforms the other approaches based on traditional machines learning techniques in terms of overall accuracy.

---

17 Marian-Daniel Iordache, José M Bioucas-Dias y Antonio Plaza. “Total variation spatial regularization for sparse hyperspectral unmixing”. En: *IEEE Transactions on Geoscience and Remote Sensing* 50.11 (2012), págs. 4484-4502.

18 Michael Eismann. “Hyperspectral remote sensing”. En: Society of Photo-Optical Instrumentation Engineers. 2012.

19 Farid Melgani y Lorenzo Bruzzone. “Classification of hyperspectral remote sensing images with support vector machines”. En: *IEEE Transactions on geoscience and remote sensing* 42.8 (2004), págs. 1778-1790.

1. OBJETIVES

General Objetive

- To design a classification approach for hyperspectral images based on convolutional neural networks and spectral unmixing.

Specific objectives

- To review of the state of the art of linear techniques for spectral unmixing of hyperspectral images and classification methods based on convolutional neural network.
- To implement a convolutional neural network architecture that performs hyperspectral classification from the spectral unmixing.
- To evaluate the proposed classification method using traditional spectral data sets.
- To compare the proposed classification approach with respect to classification techniques in the state of the art.

2. PUBLICATIONS

Some results of this work were published in the papers shown as follows:

- Pinto, Jhon E., Juan M. RamÃrez, and Henry Arguello. “Classification of oil palm diseases via spectral unmixing and convolutional neural networks.“ Remote Sensing for Agriculture, Ecosystems, and Hydrology XXI. Vol. 11149. International Society for Optics and Photonics, 2019.
- Pinto, Jhon, Hoover Rueda-Chacon, and Henry Arguello. “Classification of Hass avocado (persea americana mill) in terms of its ripening via hyperspectral images. “ TecnoLogicas 22.45 (2019): 111-130.

3. ORGANIZATION OF THE MASTER THESIS

This master thesis is organized as follows:

A background review is included in Chapter 3. More precisely, an overview of the hyperspectral imaging is introduced. Furthermore, the spectral unmixing problem in hyperspectral imaging is developed. Since the proposed approach is compared to traditional dimensionality reduction algorithms, thus, a brief description of the principal component analysis is included. Then, the main characteristics of convolutional neural networks are exposed. Finally, traditional machine learning techniques used in hyperspectral image classification are presented.

The description of the proposed classification approach based on convolutional neural networks is shown in Chapter 4. Specifically, the spectral unmixing technique implemented in the proposed approach is described. Then, a comprehensive exposure of the convolutional neural network architecture used to label hyperspectral images is introduced.

The results of numerical simulations are displayed in Chapter 5. In particular, the labeling maps obtained by the proposed classification approach are shown, as well as the accuracy results obtained by the different classifiers under test. Finally, some conclusions are summarized in Chapter 6.

4. THEORETICAL BACKGROUND

In this section, the relevant topics in the state of the art for this research work is described, such as hyperspectral imaging (HSI), spectral unmixing (SU) and convolutional neuronal networks (CNN).

4.1. HYPERSPECTRAL IMAGES

Hyperspectral remote sensing is focused on the extraction of information from objects or scenes on the Earth surface, based on their radiance acquired by airborne or spaceborne sensors [20]. Hyperspectral images (HSI) acquire spatial and spectral information of a scene, obtaining a three dimensional (3D) data cube, where two dimensions correspond to spatial coordinates (x, y) and the other corresponds to the spectral band (λ) (see figure 1). Moreover, HSI acquire from 50 to 100 bands per scene between 400 to 2500 nanometers [21] including the range Visible (VIS), Near Infrared (NIR) and Short Wave Infrared (SWIR) of the electromagnetic spectrum. HSI allow the remote identification of materials of interest based on their spectral response called spectral signature, which is a unique correspondence between a material and its reflectance spectrum [22]. HSI have been applied to numerous applications

---

[20] R Lennon. “Remote Sensing Digital Image Analysis: An Introduction”. En: *United States: Esa/Esrin* (2002).

[21] Ariolfo Camacho Velasco, César Augusto Vargas García y Henry Arguello Fuentes. “A comparative study of target detection algorithms in hyperspectral imagery applied to agricultural crops in Colombia”. En: *Tecnura* 20.49 (2016), págs. 86-99.

[22] Gary A Shaw y Hsiaohua K Burke. “Spectral imaging for remote sensing”. En: *Lincoln laboratory journal* 14.1 (2003), págs. 3-28.

including agriculture [23], [24], military defense [25], archeology [26], medical diagnosis [27], analyses of crime scene details [28], food quality control [29], mineralogical mapping of earth surface [30], among others.

4.2. SPECTRAL UNMIXING

Spectral Unmixing (SU) is a popular HSI processing technique which is used to extract land cover information and have a important use in environment, monitoring and mineral exploration. SU is the procedure used to descompose a measure from

---

[23] Megandhren Govender, K Chetty y Hartley Bulcock. "A review of hyperspectral remote sensing and its application in vegetation and water resource studies". En: *Water Sa* 33.2 (2007).

[24] Elhadi Adam, Onisimo Mutanga y Denis Rugege. "Multispectral and hyperspectral remote sensing for identification and mapping of wetland vegetation: a review". En: *Wetlands Ecology and Management* 18.3 (2010), págs. 281-296.

[25] Jean-Pierre Ardouin, Josée Lévesque y Terry A Rea. "A demonstration of hyperspectral image exploitation for military applications". En: *Information Fusion, 2007 10th International Conference on*. IEEE. 2007, págs. 1-8.

[26] Haida Liang. "Advances in multispectral and hyperspectral imaging for archaeology and art conservation". En: *Applied Physics A* 106.2 (2012), págs. 309-323.

[27] Oscar Carrasco y col. "Hyperspectral imaging applied to medical diagnoses and food safety". En: *Geo-Spatial and Temporal Image and Data Exploitation III*. Vol. 5097. International Society for Optics y Photonics. 2003, págs. 215-222.

[28] Jaana Kuula y col. "Using VIS/NIR and IR spectral cameras for detecting and separating crime scene details". En: *Sensors, and Command, Control, Communications, and Intelligence (C3I) Technologies for Homeland Security and Homeland Defense XI*. Vol. 8359. International Society for Optics y Photonics. 2012, 83590P.

[29] Yao-Ze Feng y Da-Wen Sun. "Application of hyperspectral imaging in food safety inspection and control: a review". En: *Critical reviews in food science and nutrition* 52.11 (2012), págs. 1039-1058.

[30] Roger N Clark y Gregg A Swayze. "Mapping minerals, amorphous materials, environmental materials, vegetation, water, ice and snow, and other materials: the USGS Tricorder algorithm". En: (1995).

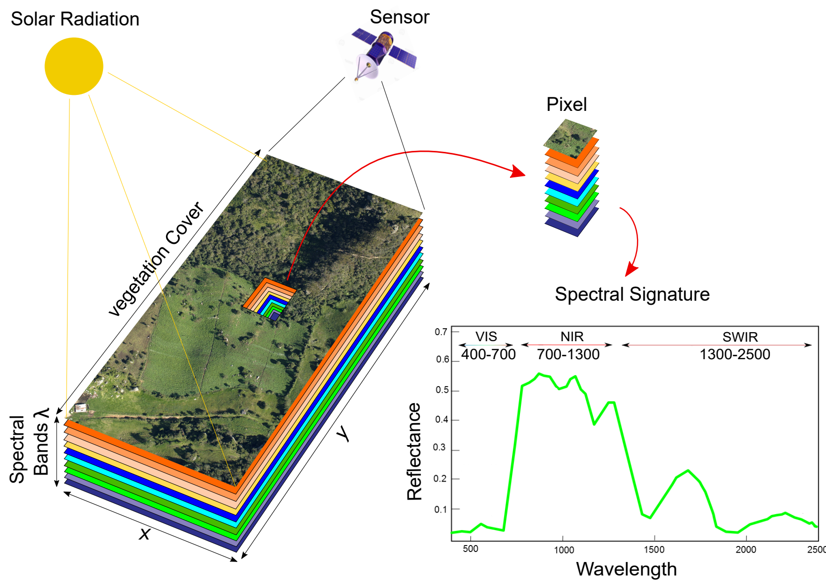

Figura 1. Representation of hyperspectral image from to remote sensing

a mixed pixel into a collection of previously known spectral signatures, or endmembers, which generally corresponds to a specific material, and a set of corresponding fractions, or abundances, that indicate the proportion of each endmember contained in the pixel [7] (see figure 2). The endmembers represent the pure materials contained in the image and the abundances represent the percentage of each endmember that is in each the pixel [31]. SU is divided into two categories, the Linear Spectral Mixture Model (LSMM) and Nonlinear Spectral Mixture Model (NLSMM). In this work, we focus in the LSMM, which assumes that spectrum of a mixed pixel is represented as a linear combination of endmembers and the abundance is proportional to the fraction of the pixel area covered by the endmember [32]. In this sense, exists a linear

[31] José M Bioucas-Dias y col. “Hyperspectral unmixing overview: Geometrical, statistical, and sparse regression-based approaches”. En: *IEEE journal of selected topics in applied earth observations and remote sensing* 5.2 (2012), págs. 354-379.

[32] John B Adams, Milton O Smith y Paul E Johnson. “Spectral mixture modeling: A new analysis of rock and soil types at the Viking Lander 1 site”. En: *Journal of Geophysical Research: Solid Earth* 91.B8 (1986), págs. 8098-8112.

relationship between the fractional abundance of the substances covering the area being imaged and the spectra in the reflected radiation [33]. In this case, LSMM can be represented mathematically as:

$$\mathbf{y}_i = \sum_{j=1}^{p} \mathbf{p}_j \alpha_{ij} + \mathbf{w}_i \tag{1}$$

where $\mathbf{y}_i$ is the $i-th$ acquired spectral signature, $\mathbf{p}_j$ represents $j-th$ endmember, α_{ij} denotes the fractional abundance of the $j-th$ endmember for building the $i-th$ measurement, and $\mathbf{w}_i$ is the noise vector. The abundances are subject to the following constraints:

- Nonnegativity assumes that abundances must be greater than or equal to zero.

$$\alpha_{ij} \geq 0, j = 1, ..., p \tag{2}$$

- Sum-to-one assumes that the sum of the abundances are equal to one.

$$\sum_{j=1}^{p} \alpha_{ij} = 1 \tag{3}$$

Finally, the expression (1) can be rewritten as

$$\mathbf{y}_i = \mathbf{P}\alpha + \mathbf{w} \tag{4}$$

where $p = [p_1, p_2, ..., p_p]$ is the mixing matrix containing the signatures of the end-members contained in the covered area.

---

[33] Dimitris Manolakis, Christina Siracusa y Gary Shaw. “Hyperspectral subpixel target detection using the linear mixing model”. En: *IEEE Transactions on Geoscience and Remote Sensing* 39.7 (2001), págs. 1392-1409.

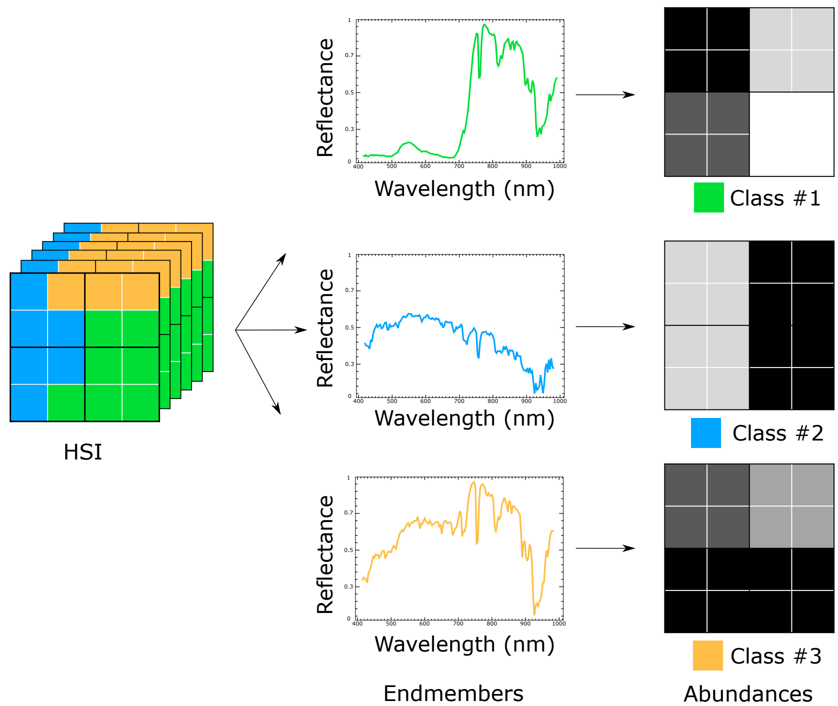

Figura 2. Representation of LSMM for three endmembers

4.3. PRINCIPAL COMPONENTS ANALYSIS

The principal component analysis (PCA) is based on the fact that neighboring bands of hyperspectral images are highly correlated and often convey almost the same information about the object. The analysis is used to transform the original data for removing the correlation among the bands. In the process, the optimum linear combination of the original bands accounting for the variation of pixel values in an image is identified.

The PCA employs the statistic properties of hyperspectral bands to examine band dependency or correlation. This is based on the same mathematical principle known as eigenvalue decomposition of the covariance matrix of the hyperspectral image bands to be analyzed [34].

4.4. CONVOLUTIONAL NEURAL NETWORKS

The CNN are a trainable multilayer architecture composed of multiple feature-extraction stages. Each stage consists of three layers: 1) a convolutional layer, 2) a nonlinearity layer and 3) a pooling layer [9]. The role of the convolutional layer is to detect local conjunctions of features from the previous layer. The input to the convolutional layer is a three-dimensional array with r two-dimensional feature maps of size m x n. Each component is denoted as $x^i_{m,n}$ and each feature map is denoted as x^i. The output is also a three dimensional array m_1 x n_1 x k, composed of k feature maps of size m_1 x n_1. The convolutional layer has k trainable filters called the filter bank W, which connects the input feature map to the output feature map. In the traditional CNN, the nonlinearity layer simply consists of a pointwise nonlinearity function applied to each component in a feature map. Finally, the role of the pooling layer is to merge semantically similar features into one is due to the relative positions of the features can vary [34]. A typical pooling unit computes the maximum of a local patch of units in one feature map or another approach is the average in the local patch. The main characteristic of a CNN is the weight sharing, which can significantly reduce the number of neural networks parameters, and thus prevent the emergence of over fitting, while reducing the complexity of the neural network model. CNN models can potentially lead to progressively more abstract and complex features at higher layers [35], in order to improve the performance in the HSI classification. Nowadays, CNN has been

---

[34] Yann LeCun, Yoshua Bengio y Geoffrey Hinton. “Deep learning”. En: *nature* 521.7553 (2015), pág. 436.

[35] Yushi Chen y col. “Deep learning-based classification of hyperspectral data”. En: *IEEE Journal of Selected topics in applied earth observations and remote sensing* 7.6 (2014), págs. 2094-2107.

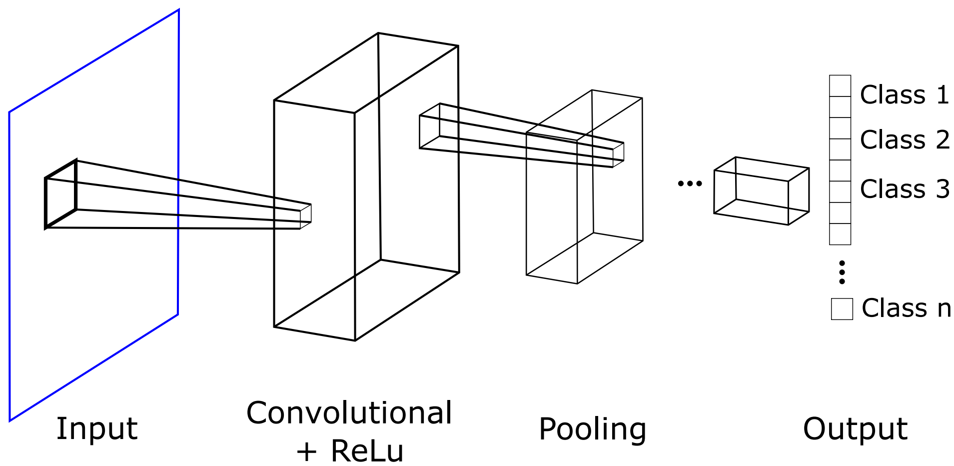

Figura 3. Representation of CNN model

applied in several applications such as: HSI classification [36], [37], face recognition [38], handwritten character classification [39]. In the figure 3 is a representation of a CNN, we can observed the input data, the convolutional layer, the nonlinearity layer and the pooling layer.

4.5. CLASSIFICATION ALGORITHMS

In this project, we use the following classifiers in order to compare our proposed method. Next, we describe each one.

---

[36] Yushi Chen y col. "Deep feature extraction and classification of hyperspectral images based on convolutional neural networks". En: *IEEE Transactions on Geoscience and Remote Sensing* 54.10 (2016), págs. 6232-6251.

[37] Konstantinos Makantasis y col. "Deep supervised learning for hyperspectral data classification through convolutional neural networks". En: *Geoscience and Remote Sensing Symposium (IGARSS), 2015 IEEE International*. IEEE. 2015, págs. 4959-4962.

[38] Steve Lawrence y col. "Face recognition: A convolutional neural-network approach". En: *IEEE transactions on neural networks* 8.1 (1997), págs. 98-113.

[39] Dan Claudiu Ciresan y col. "Convolutional neural network committees for handwritten character classification". En: *Document Analysis and Recognition (ICDAR), 2011 International Conference on*. IEEE. 2011, págs. 1135-1139.

4.5.1. Support vector machine (SVM) It is a classifier, originally proposed by Vapnik, that finds a maximal margin separating hyperplane between two classes of data [40]. This avoid the “curse of dimensionality“ by placing an upper bound on the margin between different classes. The classification problem is viewed as a quadratic optimization problem. To classify data a set of support vectors, which are members of the training data outlining the hyperplane in the feature space, is determined [41]. To describe the optimal separating hyperplane in the feature space and estimating the corresponding coefficients of expansion of separating hyperplane, the inner product of two vectors in the feature space is estimated as a function of two variables in the input space [40]. Such functions are known as kernel functions. SVMs are the most well known class of algorithms, which use the idea of kernel substitution. With suitable choice of kernel the data can become separable in the feature space despite being non separable in the input space. Some popular kernel functions is radial basis functions(RBF) [42].

4.5.2. Support vector machine-Radial Basis Function (SVM-RBF) It is one of the most popular Kernel method used in SVM models. RBF kernel is a function whose value depends on the distance from the origin or from some point. This is another shape to represent of SVM, this classifier may use kernel functions which replace the vector. In this case, the problem transforms into an equivalent linear hyper plane problem of higher (sometimes infinite) dimensionality. Commonly used

---

[40] Vladimir N Vapnik. “An overview of statistical learning theory”. En: *IEEE transactions on neural networks* 10.5 (1999), págs. 988-999.

[41] Christopher JC Burges. “A tutorial on support vector machines for pattern recognition”. En: *Data mining and knowledge discovery* 2.2 (1998), págs. 121-167.

[42] Tarun Ambwani. “Multi class support vector machine implementation to intrusion detection”. En: *Proceedings of the International Joint Conference on Neural Networks, 2003.* Vol. 3. IEEE. 2003, págs. 2300-2305.

SVM kernels include linear, polynomial, gaussian also known as radial basis function (RBF), sigmoid and normalized kernels [43].

4.5.3. K-nearest neighbors (KNN) It is one of the most fundamental and simple classification methods and should be one of the first choices for a classification study when there is little or no prior knowledge about the distribution of the data. K-nearest-neighbor classification was developed from the need to perform discriminant analysis when reliable parametric estimates of probability densities are unknown or difficult to determine. The KNN rule classifies each unlabeled example by the majority label among its k-nearest neighbors in the training set. Its performance thus depends crucially on the distance metric used to identify nearest neighbors [44].

---

[43] J Yuhendra, Hiroake Kuze y J Sri Sumantyo. "Performance analyzing of high resolution pan-sharpening techniques: increasing image quality for classification using supervised kernel support vector machine". En: *Research Journal of Information Technology* 3.1 (2011), págs. 12-23.

[44] Kilian Q Weinberger, John Blitzer y Lawrence K Saul. "Distance metric learning for large margin nearest neighbor classification". En: *Advances in neural information processing systems*. 2006, págs. 1473-1480.

5. CLASSIFICATION METHODOLOGY

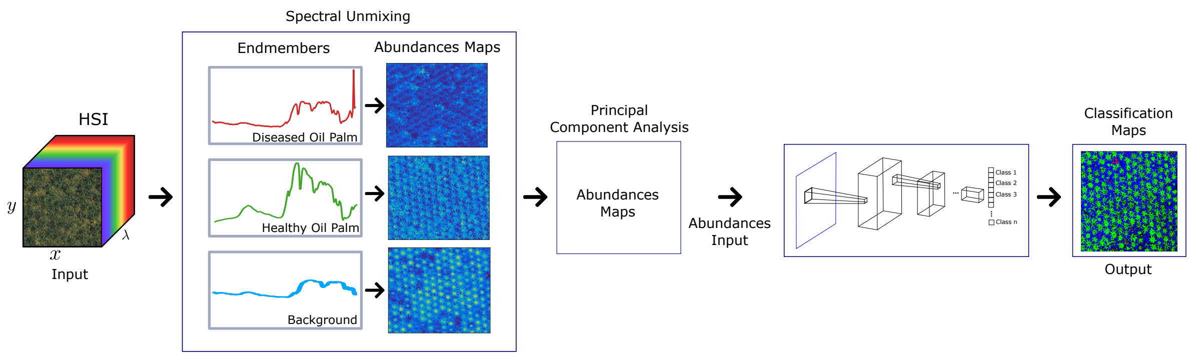

Figura 4. Proposed CNN architecture

In this chapter, the methodology to classify hyperspectral images using both a spectral unmixing (SU) method and a convolutional neural network (CNN) is introduced. Figure 4 shows the flowchart of the proposed classification method. As can be seen in this figure, both the set of endmembers and the set of abundance maps are obtained by implementing a SU method. More precisely, the sparse unmixing method via variable splitting augmented Lagrangian and total variation (SunSal-TV) is applied to the input hyperspectral image [17]. Since the SU method decomposes the hyperspectral image as a linear combination of 2-D images (abundance maps) whose spatial structure depends on a set of predefined spectral signatures (endmembers), the proposed classification approach considers both the spectral and spatial properties of the hyperspectral image under test. The principal component analysis (PCA) decomposition [45] is then applied to the set of abundance maps in order to obtain the relevant information of the hyperspectral image at sub-pixel levels. Afterward, a patch extraction procedure is performed over the set of principal components. Specifically,

[45] DF Frey y RA Pimentel. “Principal component analysis and factor analysis”. En: (1978).

for every image pixel, a cubic patch of size $5 \times 5 \times L_e$ centered at each pixel is used, where L_e denotes the number of endmembers. It is worth noting that the extracted patches contain the neighboring spatial information of each pixel, in other words, the proposed classification methodology considers the spatial-contextual information of the scene to improve the classification performance. Next, these patches are considered as the input attributes of a CNN classification architecture [46]. To be more precise, the CNN architecture comprises two convolutional layers, two nonlinear activation function layers, one max-pooling layer, and a fully-connected layer.

This chapter is organized as follows. First, the SunSal-TV algorithm and the corresponding implementation details are described. Then, the characteristics of the the implemented classification CNN architecture are shown.

5.0.1. The SunSal-TV algorithm In essence, the sparse unmixing method via variable splitting augmented Lagrangian and total variation (SunSal-TV) is an algorithm based on the sparse unmixing formulation. Notice that the sparse unmixing model describes every spectral signature as a linear combination of pure material spectra. In addition, the SunSal-TV method includes a total variation (TV) regularization to the classical sparse unmixing formulation in order to consider the spatial-contextual information embedded in hyperspectral images [17]. Hence, the SunSal-TV unmixing algorithm attempts to solve the following nonsmooth convex optimization problem

$$\underset{X}{\text{mín}}\frac{1}{2}\|\mathbf{AX}-\mathbf{Y}\|_F^2+\lambda\|\mathbf{X}\|_{1,1}+\lambda_{TV}\|\mathbf{X}\|_{TV}, \text{ subject to } \mathbf{X}\geq 0 \tag{5}$$

where $\mathbf{Y} \in \mathbb{R}^{L\times n}$ is the input hyperspectral image in matrix form (where each column contains the spectral signature of the corresponding spatial coordinate) with L as the

[46] Aurélien Géron. *Hands-on machine learning with Scikit-Learn, Keras, and TensorFlow: Concepts, tools, and techniques to build intelligent systems.* O'Reilly Media, 2019.

number of spectral bands and n as the number of pixels of the input hyperspectral image; $\mathbf{X} \in \mathbb{R}^{m \times n}$ contains the information of the abundance maps in matrix form with m denoting the number of endmembers; and $\mathbf{A} \in \mathbb{R}^{L \times m}$ is the endmember matrix. Note that $\parallel \mathbf{X} \parallel_F \equiv \sqrt{trace\,\{\mathbf{X}\mathbf{X}^\mathbf{T}\}}$ represents the Frobenius norm of $\mathbf{X}$ and $\|\mathbf{X}\|_{1,1} \equiv \sum_{i=1}^{n} \|\mathbf{x_i}\|_1$ and $\mathbf{x_i}$ denotes the i-th column of $\mathbf{X}$. Finally $\lambda \geq 0$ and $\lambda_{TV} \geq 0$ are the parameters that controls the influence of the regularization terms also known as regularization parameters. On the other hand, the total variation norm is given by

$$\|\mathbf{X}\|_{TV} \equiv \sum_{\{i,j\}\epsilon\varepsilon} \parallel \mathbf{x_i} - \mathbf{x_j} \parallel \tag{6}$$

that can be considered as an extension of the nonisotropic TV [47]. In general, the TV-norm induces regular piece-wise regions in the abundance maps, preserving in turn, the edges of the scene. This is, this norm includes the information of the set of neighboring pixels, where ε denotes the set of horizontal and vertical neighbors included in the TV-norm expression. Note also that the minimization (5) without the TV-norm term ($\lambda_{TV} = 0$) reduces to the constrained basis pursuit denoising (CBPDN) problem. In this regard, the technical documentation of the CBPDN method and other constrained sparse regression algorithms in the hyperspectral unmixing context are extensively analyzed in [48]. Furthermore, the implementation details of the SunSal-TV algorithm are comprehensively included in [17].

In particular, the SunSal-TV algorithm is selected because this method induces piece-wise smoothing regions in the obtained abundance maps. Specifically, this property considers the spatial-contextual information of the hyperspectral image that

[47] Leonid I Rudin, Stanley Osher y Emad Fatemi. “Nonlinear total variation based noise removal algorithms”. En: *Physica D: nonlinear phenomena* 60.1-4 (1992), págs. 259-268.

[48] Marian-Daniel Iordache, José M Bioucas-Dias y Antonio Plaza. “Sparse unmixing of hyperspectral data”. En: *IEEE Transactions on Geoscience and Remote Sensing* 49.6 (2011), págs. 2014-2039.

is relied on the assumption that neighboring pixels exhibit similar fractional abundaces. Additionally, this characteristic also allows to improve the performance of the pixel-based classification techniques. In this regard, we use the matlab code of the SunSal-TV unmixing algorithm available in [49]. For each input hyperspectral image database, the SunSal-TV algorithm is executed, where the number of endmembers is set same as the number of classes of the ground-truth labelling map. Furthermore, for each hyperspectral image database, the best regularization parameters is selected by cross-validation whose selection criterion was the Frobenious norm of the representation error. Finally, the set of abundance maps of the corresponding hyperspectral image is stored in .MAT format in order to use this information in a Python programming environment.

5.0.2. The implemented CNN architecture The MAT file that contains the set of abundance maps obtained by the SunSal-TV algorithm is loaded to implement the spectral image classification approach. Specifically, this spectral image classification approach is implemented in the Jupyter Notebook framework. Afterward, the abundance map datacube $\mathcal{X} \in \mathbb{R}^{M\times N\times L_e}$ is considered as the input of a PCA decomposition function, where $M \times N$ is the number of pixels and L_e is the number of endmembers. This decomposition generates a datacube $\mathcal{X}_{PCA} \in \mathbb{R}^{M\times N\times L_e}$. Note that the PCA decomposition is typically implemented in spectral image classification problems to improve the labelling accuracy. Then, a patch extraction procedure is applied to each spatial coordinate of the PCA decomposition. To be more precise, for each spatial coordinate, a patch with size $5\times 5\times L_e$ centered at the corresponding pixel is obtained. Every patch is then used as the input of a CNN architecture that implements a pixel-based classification.

[49] `http://www.lx.it.pt/ bioucas/publications.html.`

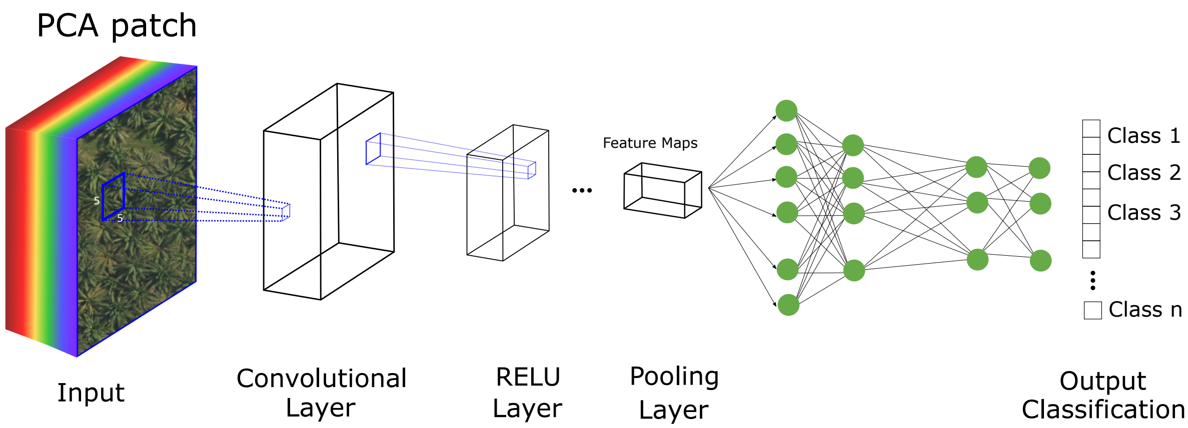

Figura 5. Proposed CNN architecture

Figure 5 illustrates a schematic of the implemented CNN architecture for hyperspectral image classification. As can be seen in this figure, each input patch feeds a convolutional layer that consists of L_e filters of size 3×3, the stride is set to 1, and there is no padding. Then, the output of the convolutional layer is activated with a rectified linear unit (ReLU) which is defined as $f(u) = \max(u, 0)$. The dimensions of the features are reduced by implementing a max-pooling function with kernel stride of 2. Afterward, a convolutional layer with $3L_e$ filters with dimensions 3×3 with stride fixed to one, and no padding. A ReLU activation function and a max-pooling layer are also included. Finally, a fully-connected multilayer perceptron neural network (MLPNN) is aggregated.

To be more precise, three fully-connected layers were added at the output end of the CNN. Specifically, the output of the j-th node at the k-th layer outputs can be expressed as

$$\zeta_j^k = \mathrm{ReLU}\left(\sum_{i=1}^{N_n} \Upsilon_{i,j}^{k-1} \zeta_{i,j}^{k-1} + \xi_j^{k-1}\right) \tag{7}$$

where $\Upsilon_{i,j}^{k-1}$ is the coefficient that connects the i-th node at the $k-1$ layer with the j-th node in layer k, and ξ_j^{k-1} is the bias term of the j-th node in layer k. In this work, we select number of hidden layers by implementing a classification performance search. The output layer size depends on the number of the classes and the network parameters are updated by using the back-propagation algorithm with the binary cross-entropy loss function.

Basically, the fully-connected structure attempts to learn the network parameter set $\boldsymbol{\Theta} = \{\boldsymbol{\Upsilon}, \boldsymbol{\xi}\}$ that basically contains the connection weight matrix $\boldsymbol{\Upsilon}$ and the bias vector $\boldsymbol{\xi}$. Under the multiclass classification framework, consider $\mathbf{z}_n \in \{0,1\}^{N_c}$ as the n-th ground truth label vector with N_c as the number of output classes, and let s_n be the corresponding input vector, therefore, the training set can be represented as $\Gamma = \{\mathbf{z}_n, \mathbf{s}_n\}_{n=1}^{N_t}$ with N_t as the number of training samples. Hence, the training stage attempts learn the network parameters $\boldsymbol{\Theta}$ that minimize the cross-entropy loss function given by

$$\mathcal{E}(\boldsymbol{\Theta}) = -\sum_{n=1}^{N_t}\sum_{c=1}^{N_c}(\mathbf{z}_n)_c \log\left((\mathbf{p}_n(\boldsymbol{\Theta}, \mathbf{s}_n))_c\right) \tag{8}$$

where $(\mathbf{z}_n)_c$ is the c-th element of the ground truth label vector and $(\mathbf{p}_n(\boldsymbol{\Theta}, \mathrm{s}_n))_c$ is the probability predicted by the network at the c-th output layer node. Notice that the network parameters are randomly initialized.

Algorithm 1 illustrates the steps of the proposed hyperspectral image classification method.

Algorithm 1 Proposed classification approach

procedure Class_HS($\mathbf{Y} \rightarrow$ input hyperspectral image)
$[\mathbf{A}, \mathbf{X}] = \mathrm{SunSal} - \mathrm{TV}(\mathbf{Y})$
$\mathcal{X}_{PCA} = \mathrm{PCA}(\mathbf{X})$
`PATCH_SIZE` $\rightarrow 5 \times 5 \times L_e$
$\mathcal{X}_{patch} = \mathrm{Patch\_Extraction}(\mathcal{X}_{PCA})$
`MAX_EPOCHS` $\rightarrow$ Set the number of epochs
`MAX_ITER` $\rightarrow$ Set the number of iterations
`BATCH_SIZE` $\rightarrow$ Set the batch size
$\Gamma = \{\mathbf{z}_n, \mathbf{s}_n\}_{n=1}^{N_t} \rightarrow$ Training set
$G = \mathrm{Batch\_Building}(\Gamma,$`BATCH_SIZE`$)$
for $e <$ `MAX_EPOCHS` **do**
    for $it <$ `MAX_ITER` **do**
        $G' = \mathrm{get\_next\_batch}(G)$
        forward_pass(G')
        $\mathcal{E}(\mathbf{\Theta}) = -\sum_{n=1}^{N_t} \sum_{c=1}^{N_c} (\mathbf{z}_n)_c \log\left((\mathbf{p}_n(\mathbf{\Theta}, \mathbf{s}_n))_c\right)$
        $CNN_{parameters} = optimize(\mathcal{E}(\mathbf{\Theta}))$
    end for
end for
end procedure

6. EXPERIMENTAL RESULTS

In this section, it presents the experimental results of the final stage of the methodology proposed on different datasets, also, we add a brief description of each one.

6.1. DATASET

Next, each of the datasets used in the research work is described.

6.1.1. Indian Pine This scene was gathered by AVIRIS sensor over the Indian Pines test site in North-western Indiana and consists of 145*145 pixels and 224 spectral reflectance bands in the wavelength range $0.4-2.5\ 10^{(-6)}$ meters. This scene is a subset of a larger one. The Indian Pines scene contains two-thirds agriculture, and one-third forest or other natural perennial vegetation. There are two major dual lane highways, a rail line, as well as some low density housing, other built structures, and smaller roads. Since the scene is taken in June some of the crops present, corn, soybeans, are in early stages of growth with less than 5 % coverage. The ground truth available is designated into sixteen classes and is not all mutually exclusive. We have also reduced the number of bands to 200 by removing bands covering the region of water absorption: [104-108], [150-163], 220.

6.1.2. Pavia University This scene was acquired by the ROSIS sensor during a flight campaign over Pavia, nothern Italy. The number of spectral bands is 103 for Pavia University. Pavia University is 610×610 pixels, but some of the samples contain no information and have to be discarded before the analysis. The geometric resolution is 1.3 meters. The groundtruth differenciate 9 classes each. It can be seen the discarded samples in the figures as abroad black strips. Pavia scene were provided by Prof. Paolo Gamba from the Telecommunications and Remote Sensing Laboratory, Pavia university (Italy).

6.1.3. Salinas Valley This scene was collected by the 224-band AVIRIS sensor over Salinas Valley, California, and is characterized by high spatial resolution (3.7-meter pixels). The area covered comprises 512 lines by 217 samples. As with Indian Pines scene, we discarded the 20 water absorption bands, in this case bands: [108-112], [154-167], 224. This image was available only as at-sensor radiance data. It includes vegetables, bare soils, and vineyard fields. Salinas groundtruth contains 16 classes.

6.1.4. Oil Palm The data set Oil Palm was collected in 2017 by HySpex VNIR-1600 hyperspectral camera which recorded the remote sensing images in eastern region Caqueta, Colombia. The hyperspectral image of the oil palm crop was got thanks to a Colombian company called *Quimbaya Aerial Services*, this image contains 299×294 pixels in spatial dimensions and 160 hyperspectral bands which have a range spectral from 400 nanometers to 1000 nanometers, the study area is a crop of 130 hectares, the hyperspectral image was acquired through nine flight lines and 430 meters of flight altitude. On the other hand, the ground truth was manually created with 3 classes such as, diseased plants in color red, healthy plants in color green, and background in color blue, where the location of diseased oil palm plants were taking control points with a GPS.

6.2. SIMULATIONS RESULTS

Several simulations were performed to test the performance of the proposed method using traditional hyperspectral datasets available on the web. The numerical results and simulations were performed in Python using Tensor Flow with the library Keras;

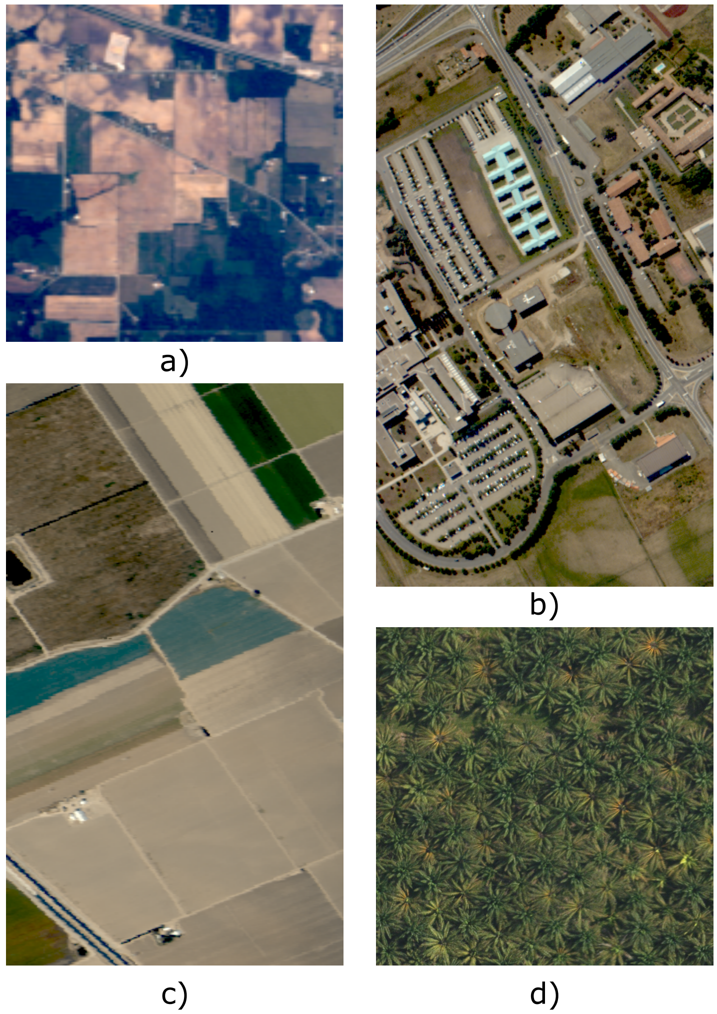

Figura 6. Spectral images dataset used a) Indian Pine, b) Pavia University, c) Salinas Valley, d) Oil Palm Crop

and MatLab. These experiments were carried out on a computer with a processor Intel(R) core (TM) i7-6700 CPU @ 3.40GHz and the 16 GB of RAM memory.

In this simulations, we classify the different class by each dataset, we use the abundances maps of each dataset as input to CNN, also, we choose randomly the pixels for training (10 %, 15 % and 20 %) and validation (90 %, 85 % and 80 %). The abundances maps were generated using the algorithm of spectral unmixing called SUn-SAL TV [17] where estimated different endmembers with its respective abundances maps according to the dataset, these endmembers were verified with the pure spectral signature in the hyperspectral image.

Next, we have visual maps of the proposed method and the other traditional methods that we used to compare our approach such as support vector machine (SVM), SVM-Radial Basis Function (RBF) and K-nearest neighbors (KNN), also, we can see different visual maps where we alter different training data, and on the other hand, we can see the quantitative results of each dataset with its different varying.

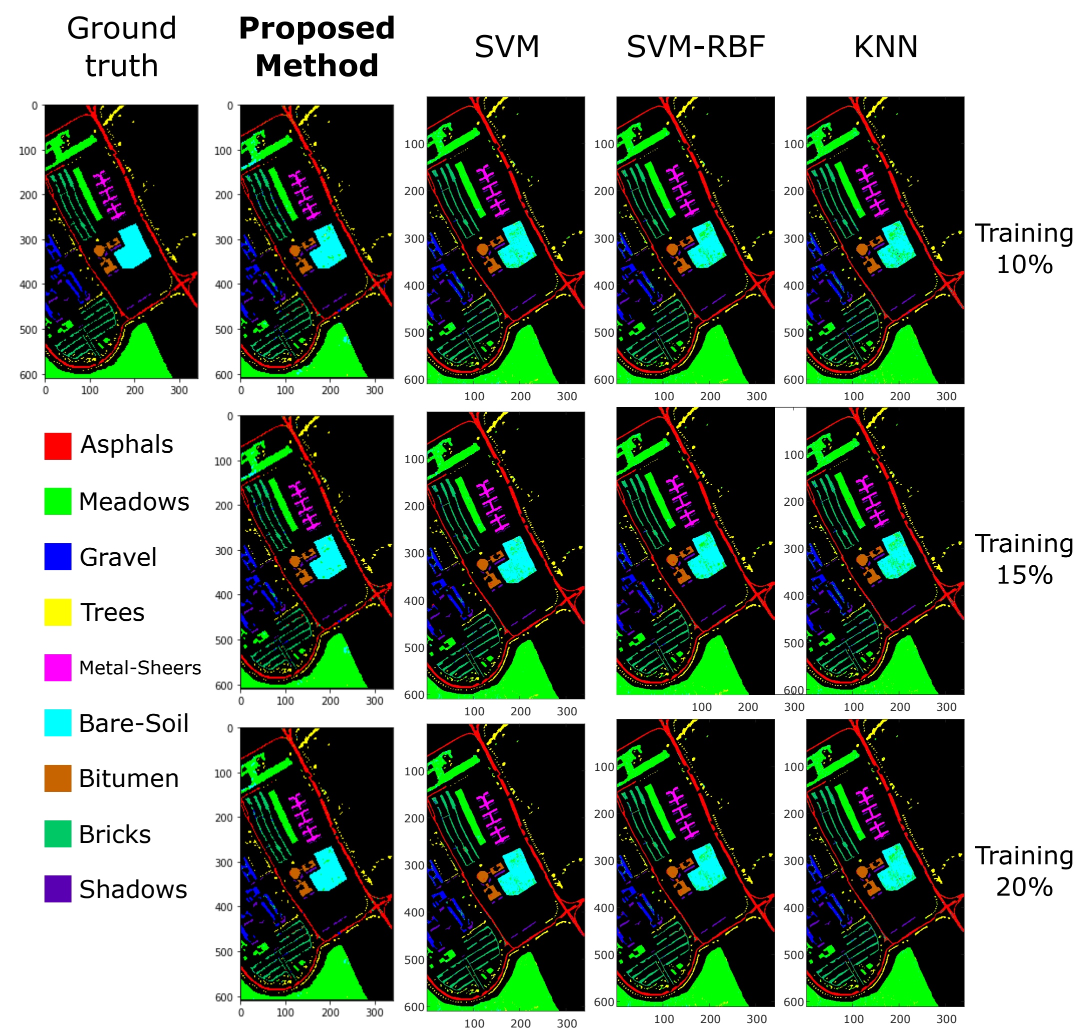

Figura 7. Visual maps with classification results using the abundances of Pavia University dataset with training data 10 %, 15 %, and 20 % and its ground truth.

The quantitative results are shown in table 1 which presents the classification accuracy percentage of our experiments. Notice that the proposed method presents better accuracy at each training data distribution than traditional classification approaches. To 20 % training, we got 98.9967 percentage accuracy. To 15 % training, we got 98.8544 percentage accuracy and finally, to 10 % training, we got 98.6013 percentage accuracy.

Pavia University	**Accuracy**		
	10 % Training	**15 % Training**	**20 % Training**
Proposed Method	**98.6013**	**98.8544**	**98.9667**
SVM	93.5835	94.2703	94.684
SVM-RBF	93.7732	94.1273	94.2106
KNN	91.6378	92.0643	92.6851

Tabla 1. Quantitative results on Pavia University dataset

The quantitative results are shown in table 2 which present the classification accuracy of our experiments. Notice that the proposed method presents better accuracy at each training data distribution than traditional classification approaches.To 20 % training, we got 99.2402 percentage accuracy. To 15 % training, we got 98.9893 percentage accuracy and finally, to 10 % training, we got 98.5795 percentage accuracy.

Salinas Valley	**Accuracy**		
	10 % Training	**15 % Training**	**20 % Training**
Proposed Method	**98.5795**	**98.9893**	**99.2402**
SVM	98.1069	98.463	98.5334
SVM-RBF	98.0556	98.2793	98.3391
KNN	98.1706	98.3326	98.5311

Tabla 2. Quantitative results on Salinas Valley dataset

The quantitative results are shown in table 3 which present the classification accuracy of our experiments. Notice that the proposed method presents better accuracy at each training data distribution than traditional classification approaches. To 20 %

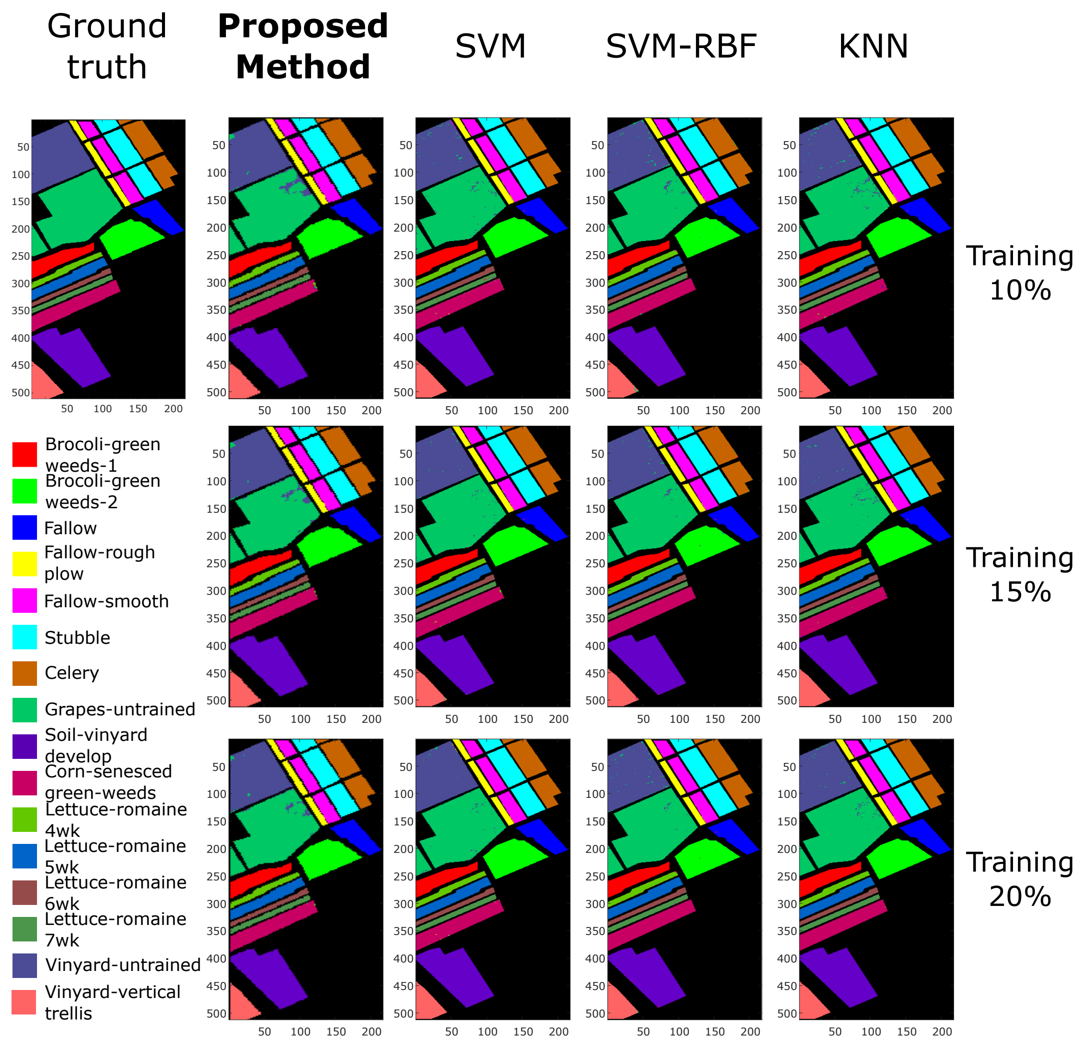

Figura 8. Visual maps with classification results using the abundances of Salinas dataset with training data 10 %, 15 %, and 20 % and its ground truth.

training, we got 94.4257 percentage accuracy. To 15 % training, we got 93.1367 percentage accuracy and finally, to 10 % training, we got 91.4102 percentage accuracy. Finally, we used our proposed method using data of Oil Palm, in this experiment, we classified diseases and healthy plants.

The quantitative results are shown in table 4 which present the classification accuracy of our experiment. Notice that the proposed method presents better accuracy at each training data distribution than traditional classification approaches. To 20 %

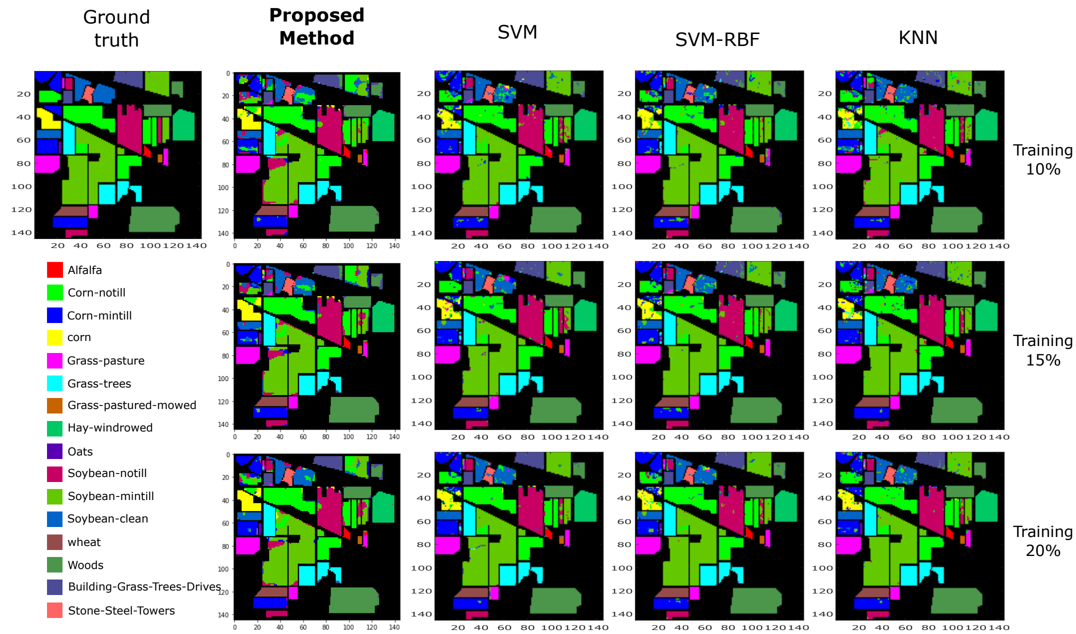

Figura 9. Visual maps with classification results using the abundances of Indian Pine dataset with training data 10 %, 15 %, and 20 % and its ground truth.

Indian Pine	Accuracy		
	10 % Training	15 % Training	20 % Training
Proposed Method	**91.4102**	**93.1367**	**94.4257**
SVM	90.8136	89.7978	90.782
SVM-RBF	84.2023	87.9878	93.2852
KNN	87.6933	92.7966	93.5325

Tabla 3. Quantitative results on Indian Pine dataset

training, we got 88.7861 percentage accuracy. To 15 % training, we got 87.1479 percentage accuracy and finally, to 10 % training, we got 84.5312 percentage accuracy.

Oil Palm	Accuracy		
	10 % Training	15 % Training	20 % Training
Proposed Method	**84.5312**	**87.1479**	**88.7861**
SVM	77.1572	77.2696	77.4516
SVM-RBF	78.3314	78.4755	78.5848
KNN	70.4633	70.5281	70.7016

Tabla 4. Quantitative results on Oil Palm dataset

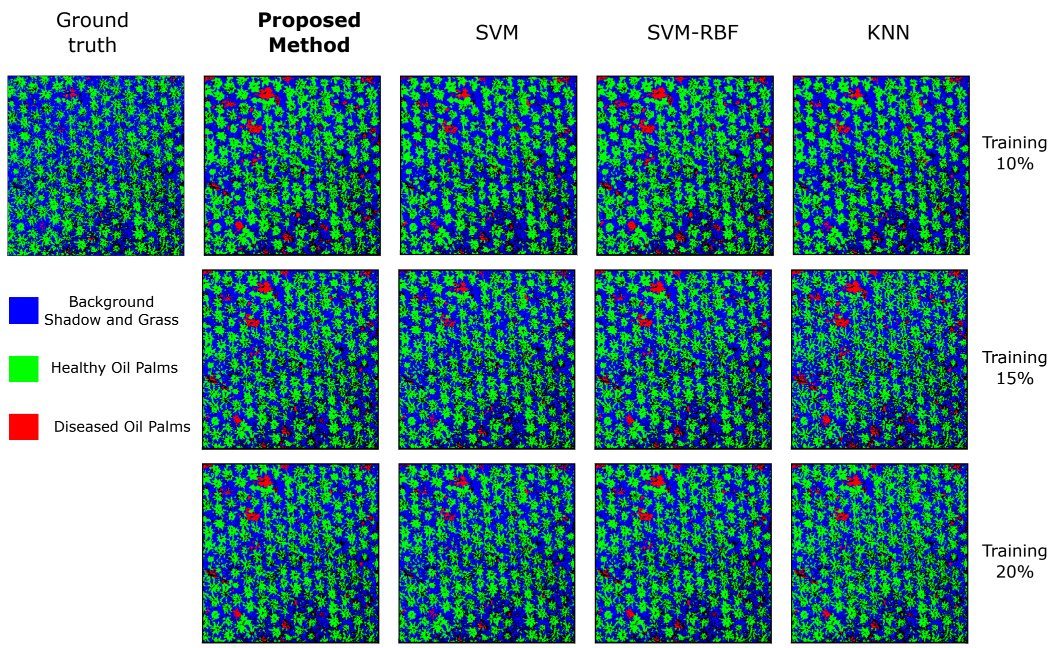

Figura 10. Visual maps with classification results using the abundances of Oil Palm dataset with training data 10 %, 15 %, and 20 % and its ground truth.

7. CONCLUSIONS

- A classification approach using a convolutional neural network that includes the abundances maps of hyperspectral images as input is proposed. Simulation results show that is possible to classify different traditional datasets and experimental dataset, for instance, a palm oil crop dataset. Additionally, the classification results obtained by the proposed method, achieve better overall accuracy than traditional approaches. In particular, to the Indian Pine, Pavia University, Salinas Vally, and Oil palm datasets, the proposed method obtains 94.4257, 98.9667, 99.2402, and 88.7861 percent of accuracy, respectively, when the 20 percent of the data is used for the training stage. Finally, one of the advantages the most important of spectral image classification is that it allows the characterization of different types of crops, therefore, the proposed convolutional neural network approach can be used to monitor and manage the plantations of the farmers in Colombia and in other countries in order to control the disease or plagues.

BIBLIOGRAPHY

Adam, Elhadi, Onisimo Mutanga y Denis Rugege. "Multispectral and hyperspectral remote sensing for identification and mapping of wetland vegetation: a review". En: *Wetlands Ecology and Management* 18.3 (2010), págs. 281-296 (vid. pág. 23).

Adams, John B, Milton O Smith y Paul E Johnson. "Spectral mixture modeling: A new analysis of rock and soil types at the Viking Lander 1 site". En: *Journal of Geophysical Research: Solid Earth* 91.B8 (1986), págs. 8098-8112 (vid. pág. 24).

Ambwani, Tarun. "Multi class support vector machine implementation to intrusion detection". En: *Proceedings of the International Joint Conference on Neural Networks, 2003.* Vol. 3. IEEE. 2003, págs. 2300-2305 (vid. pág. 29).

Ardouin, Jean-Pierre, Josée Lévesque y Terry A Rea. "A demonstration of hyperspectral image exploitation for military applications". En: *Information Fusion, 2007 10th International Conference on*. IEEE. 2007, págs. 1-8 (vid. pág. 23).

Bedini, Enton y Thorkild M Rasmussen. "Use of airborne hyperspectral and gamma-ray spectroscopy data for mineral exploration at the Sarfartoq carbonatite complex, southern West Greenland". En: *Geosciences Journal* (2018), págs. 1-11 (vid. pág. 15).

Bioucas-Dias, José M y col. "Hyperspectral unmixing overview: Geometrical, statistical, and sparse regression-based approaches". En: *IEEE journal of selected topics in applied earth observations and remote sensing* 5.2 (2012), págs. 354-379 (vid. pág. 24).

Burges, Christopher JC. “A tutorial on support vector machines for pattern recognition”. En: *Data mining and knowledge discovery* 2.2 (1998), págs. 121-167 (vid. pág. 29).

Camacho Velasco, Ariolfo, César Augusto Vargas García y Henry Arguello Fuentes. “A comparative study of target detection algorithms in hyperspectral imagery applied to agricultural crops in Colombia”. En: *Tecnura* 20.49 (2016), págs. 86-99 (vid. pág. 22).

Camps-Valls, Gustavo y col. “Advances in hyperspectral image classification: Earth monitoring with statistical learning methods”. En: *IEEE signal processing magazine* 31.1 (2013), págs. 45-54 (vid. pág. 15).

Camps-Valls, Gustavo y col. “Remote sensing image processing”. En: *Synthesis Lectures on Image, Video, and Multimedia Processing* 5.1 (2011), págs. 1-192 (vid. pág. 15).

Carrasco, Oscar y col. “Hyperspectral imaging applied to medical diagnoses and food safety”. En: *Geo-Spatial and Temporal Image and Data Exploitation III*. Vol. 5097. International Society for Optics y Photonics. 2003, págs. 215-222 (vid. pág. 23).

Chabrillat, Sabine y col. “Use of hyperspectral images in the identification and mapping of expansive clay soils and the role of spatial resolution”. En: *Remote sensing of Environment* 82.2-3 (2002), págs. 431-445 (vid. pág. 15).

Chen, Yushi y col. “Deep feature extraction and classification of hyperspectral images based on convolutional neural networks”. En: *IEEE Transactions on Geoscience and Remote Sensing* 54.10 (2016), págs. 6232-6251 (vid. pág. 28).

Chen, Yushi y col. “Deep learning-based classification of hyperspectral data”. En: *IEEE Journal of Selected topics in applied earth observations and remote sensing* 7.6 (2014), págs. 2094-2107 (vid. pág. 27).

Cireşan, Dan, Ueli Meier y Jürgen Schmidhuber. “Multi-column deep neural networks for image classification”. En: *arXiv preprint arXiv:1202.2745* (2012) (vid. pág. 17).

Ciresan, Dan Claudiu y col. “Convolutional neural network committees for handwritten character classification”. En: *Document Analysis and Recognition (ICDAR), 2011 International Conference on*. IEEE. 2011, págs. 1135-1139 (vid. pág. 28).

Clark, Roger N y Gregg A Swayze. “Mapping minerals, amorphous materials, environmental materials, vegetation, water, ice and snow, and other materials: the USGS Tricorder algorithm”. En: (1995) (vid. pág. 23).

Eismann, Michael. “Hyperspectral remote sensing”. En: Society of Photo-Optical Instrumentation Engineers. 2012 (vid. pág. 18).

Farabet, Clement y col. “Learning hierarchical features for scene labeling”. En: *IEEE transactions on pattern analysis and machine intelligence* 35.8 (2013), págs. 1915-1929 (vid. pág. 17).

Feng, Yao-Ze y Da-Wen Sun. “Application of hyperspectral imaging in food safety inspection and control: a review”. En: *Critical reviews in food science and nutrition* 52.11 (2012), págs. 1039-1058 (vid. pág. 23).

Frey, DF y RA Pimentel. “Principal component analysis and factor analysis”. En: (1978) (vid. pág. 31).

Géron, Aurélien. *Hands-on machine learning with Scikit-Learn, Keras, and TensorFlow: Concepts, tools, and techniques to build intelligent systems*. O'Reilly Media, 2019 (vid. pág. 32).

Ghamisi, Pedram y col. "Advances in hyperspectral image and signal processing: A comprehensive overview of the state of the art". En: *IEEE Geoscience and Remote Sensing Magazine* 5.4 (2017), págs. 37-78 (vid. pág. 15).

Girshick, Ross y col. "Rich feature hierarchies for accurate object detection and semantic segmentation". En: *Proceedings of the IEEE conference on computer vision and pattern recognition*. 2014, págs. 580-587 (vid. pág. 17).

Govender, Megandhren, K Chetty y Hartley Bulcock. "A review of hyperspectral remote sensing and its application in vegetation and water resource studies". En: *Water Sa* 33.2 (2007) (vid. pág. 23).

Iordache, Marian-Daniel, José M Bioucas-Dias y Antonio Plaza. "Sparse unmixing of hyperspectral data". En: *IEEE Transactions on Geoscience and Remote Sensing* 49.6 (2011), págs. 2014-2039 (vid. pág. 33).

— "Total variation spatial regularization for sparse hyperspectral unmixing". En: *IEEE Transactions on Geoscience and Remote Sensing* 50.11 (2012), págs. 4484-4502 (vid. págs. 18, 31-33, 40).

Keshava, Nirmal y John F Mustard. "Spectral unmixing". En: *IEEE signal processing magazine* 19.1 (2002), págs. 44-57 (vid. págs. 16, 24).

Krizhevsky, Alex, Ilya Sutskever y Geoffrey E Hinton. "Imagenet classification with deep convolutional neural networks". En: *Advances in neural information processing systems*. 2012, págs. 1097-1105 (vid. pág. 17).

Kuula, Jaana y col. “Using VIS/NIR and IR spectral cameras for detecting and separating crime scene details”. En: *Sensors, and Command, Control, Communications, and Intelligence (C3I) Technologies for Homeland Security and Homeland Defense XI*. Vol. 8359. International Society for Optics y Photonics. 2012, 83590P (vid. pág. 23).

Lawrence, Steve y col. “Face recognition: A convolutional neural-network approach”. En: *IEEE transactions on neural networks* 8.1 (1997), págs. 98-113 (vid. pág. 28).

LeCun, Yann, Yoshua Bengio y Geoffrey Hinton. “Deep learning”. En: *nature* 521.7553 (2015), pág. 436 (vid. pág. 27).

Lennon, R. “Remote Sensing Digital Image Analysis: An Introduction”. En: *United States: Esa/Esrin* (2002) (vid. pág. 22).

Liang, Haida. “Advances in multispectral and hyperspectral imaging for archaeology and art conservation”. En: *Applied Physics A* 106.2 (2012), págs. 309-323 (vid. pág. 23).

Makantasis, Konstantinos y col. “Deep supervised learning for hyperspectral data classification through convolutional neural networks”. En: *Geoscience and Remote Sensing Symposium (IGARSS), 2015 IEEE International*. IEEE. 2015, págs. 4959-4962 (vid. pág. 28).

Manolakis, Dimitris, Christina Siracusa y Gary Shaw. “Hyperspectral subpixel target detection using the linear mixing model”. En: *IEEE Transactions on Geoscience and Remote Sensing* 39.7 (2001), págs. 1392-1409 (vid. pág. 25).

Melgani, Farid y Lorenzo Bruzzone. “Classification of hyperspectral remote sensing images with support vector machines”. En: *IEEE Transactions on geoscience and remote sensing* 42.8 (2004), págs. 1778-1790 (vid. pág. 18).

Paoletti, ME y col. “A new deep convolutional neural network for fast hyperspectral image classification”. En: *ISPRS Journal of Photogrammetry and Remote Sensing* 145 (2018), págs. 120-147 (vid. pág. 17).

Ravikanth, Lankapalli y col. “Extraction of spectral information from hyperspectral data and application of hyperspectral imaging for food and agricultural products”. En: *Food and Bioprocess Technology* 10.1 (2017), págs. 1-33 (vid. pág. 15).

Rudin, Leonid I, Stanley Osher y Emad Fatemi. “Nonlinear total variation based noise removal algorithms”. En: *Physica D: nonlinear phenomena* 60.1-4 (1992), págs. 259-268 (vid. pág. 33).

Sermanet, Pierre, Soumith Chintala y Yann LeCun. “Convolutional neural networks applied to house numbers digit classification”. En: *Pattern Recognition (ICPR), 2012 21st International Conference on*. IEEE. 2012, págs. 3288-3291 (vid. pág. 17).

Sermanet, Pierre y Yann LeCun. “Traffic sign recognition with multi-scale convolutional networks”. En: *Neural Networks (IJCNN), The 2011 International Joint Conference on*. IEEE. 2011, págs. 2809-2813 (vid. pág. 17).

Shaw, Gary A y Hsiaohua K Burke. “Spectral imaging for remote sensing”. En: *Lincoln laboratory journal* 14.1 (2003), págs. 3-28 (vid. pág. 22).

Taigman, Yaniv y col. “Deepface: Closing the gap to human-level performance in face verification”. En: *Proceedings of the IEEE conference on computer vision and pattern recognition*. 2014, págs. 1701-1708 (vid. pág. 17).

Vapnik, Vladimir N. “An overview of statistical learning theory”. En: *IEEE transactions on neural networks* 10.5 (1999), págs. 988-999 (vid. pág. 29).

Weinberger, Kilian Q, John Blitzer y Lawrence K Saul. “Distance metric learning for large margin nearest neighbor classification”. En: *Advances in neural information processing systems*. 2006, págs. 1473-1480 (vid. pág. 30).

Yuhendra, J, Hiroake Kuze y J Sri Sumantyo. “Performance analyzing of high resolution pan-sharpening techniques: increasing image quality for classification using supervised kernel support vector machine”. En: *Research Journal of Information Technology* 3.1 (2011), págs. 12-23 (vid. pág. 30).

Zhang, Liangpei, Lefei Zhang y Bo Du. “Deep learning for remote sensing data: A technical tutorial on the state of the art”. En: *IEEE Geoscience and Remote Sensing Magazine* 4.2 (2016), págs. 22-40 (vid. págs. 17, 27).